Stabilizing Properties of Copolymers Adsorbed on Heterogeneous Surfaces: A Model for the Interactions between a Polymer-Coated Influenza Virus and a Cell

Anna C. Balazs,* Chandralekha Singh, and Ekaterina Zhulina

Department of Chemical and Petroleum Engineering, The University of Pittsburgh, Pittsburgh, Pennsylvania 15261

Received April 21, 1998; Revised Manuscript Received June 23, 1998

ABSTRACT: We use scaling theory and two-dimensional self-consistent field calculations to investigate the adsorption of copolymers onto heterogeneous surfaces, which represent the surface of the influenza virus. The copolymers contain "stickers" that are highly attracted to receptors on the viral surface. We vary the sticker concentration and determine the conformation of the adsorbed chains on the heterogeneous substrate. We then calculate the interaction energy as a function of distance between this polymer-coated surface and a bare interface, which represents the surface of a red blood cell. The results show that there is an optimal range of the sticker concentrations that sterically inhibit contact between the two surfaces. The findings help rationalize recent experiments, which show that the extent of inhibition depends on the fraction of stickers in adsorbing copolymer.

Introduction

Steric stabilization of colloids in solution can be accomplished by adsorbing polymers onto the surface of these particles.[1] As the coated particles approach each other (or an uncoated surface), segments of the adsorbed chains become compressed. This compression not only is entropically unfavorable but also increases the osmotic pressure in the region between the surfaces. As a consequence, the particles experience an effective repulsion as they come into close contact. The repulsive force prevents the particles from aggregating and thereby stabilizes the suspension. It is commonly believed that for polymers to be effective in this application, the chains must contain both a sizable solvophobic segment and a long solvophilic block.[1] The solvophobic segment effectively anchors the chains onto the surface of the colloid. The long solvophilic block extends into the solution and provides the protective layer. In this paper, we use scaling theory and self-consistent field calculations to investigate if copolymers with other types of compositions can provide effective steric stabilization of colloidal suspensions.

The particular copolymers we investigate contain a fraction of "sticker" sites along the length of the linear chains. The stickers represent solvophobic sites or specific chemical units that are highly attracted to the surface of the colloidal particle. In addition, we assume that the surface of the colloidal particle is chemically heterogeneous. Our surface contains two types of species: binding sites (or receptors) and nonreactive sites. The stickers can only bind to the surface through the receptor sites. There are two reasons why we consider such heterogeneous surfaces. First, few real surfaces are chemically homogeneous, and thus, it is important to understand how the heterogeneities on the surface affect the adsorption process. Second, as we explain below, our substrate represents a simplified model of the influenza virus. Thus, our studies are also relevant to understanding the interaction of polymers with biologically active colloids.

The influenza virus is roughly spherical in shape and is approximately 1000 Å in diameter.[2] The outer surface of the virus contains the protein hemagglutinin (HA). The HA molecules aggregate into triangular clusters.[3,4] The center-to-center distance between the clusters is 95−150 Å, and these clusters appear to be distributed irregularly on the surface of the virus. Infection of a red blood cell by influenza virus is initiated by the binding of the HA's to sialic acid (SA) groups located in glycoproteins and glycolipids on the surface of the cell. Once bound to the red blood cell, the viral interactions drive the cells to aggregate into massive clusters; this virus-mediated aggregation is referred to as hemagglutination.

Natural and synthetic macromolecules containing SA groups are effective at inhibiting the binding of virus to erythrocytes.[5−9] A possible explanation for why the SA-containing polymers inhibit binding of the virus to the cell proceeds as follows.[9] First, the polymer attaches to the viral surface through the interactions between SA and HA (see Figure 1). A substantial fraction of the HA sites remain unoccupied, and inhibition of binding of virus to cell would arise from the formation of a loosely attached, water-swollen polymer layer on the viral surface. The specific mechanism for inhibiting viral adhesion to cells would be analogous to the inhibition of aggregation of colloidal particles by adsorbed polymers, namely steric stabilization.

Experimentally, the system that has been examined consists of polyacrylamides with pendant SA groups.[5,6] The ability of the given number of SA groups attached to the polymer to inhibit the hemagglutination of the red blood cells can be 10^4 greater than the same number of SA groups free in solution. Furthermore, the fraction of SA sites within the polymer chain has a dramatic effect on the ability of the polymers to inhibit hemagglutination. Plots showing the inhibition of hemagglutination vs of fraction of SA sites within the chains have a bell-shaped appearance: at both low and high con-

* To whom correspondence should be addressed.

S0024-9297(98)00624-X CCC: $15.00
Published on Web 08/19/1998

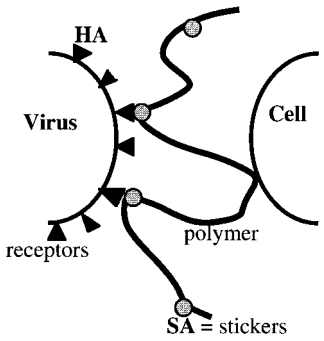

Figure 1. Schematic drawing of the interactions between a polymer-coated virus and a cell. The triangular sites represent the HA receptors on the viral surface. The circles on the chain mark the sialic acid groups within the polymer. These units are the stickers that bind to the viral receptors, or HA sites. The anchored polymer sterically inhibits contact between the particles. The different components are not drawn to scale.

centrations of SA, the effectiveness of the chains is significantly decreased.[5] Thus, for fixed molecular weight polymers, there is a optimal range of SA concentrations for producing strong inhibition.

To investigate the role of the SA concentration in inhibiting viral attachment, we first consider the more general problem of how copolymers containing various concentrations of stickers adsorb onto heterogeneous surfaces. Here, the stickers model the SA units in the synthetic polymers and the binding sites on the heterogeneous surface represent the HA receptors. Next, we examine the interaction of the polymer-coated interface with a bare surface. From these studies, we relate the concentration of stickers within the chains to the ability of the bound copolymers to sterically hinder the aggregation of the two surfaces. Finally, we discuss the implications of our findings for the interactions between polymer-coated viruses and cells.

To carry out these investigations, we construct a simple scaling model and then use a two- dimensional self-consistent field theory (SCF) to test the predictions from the scaling theory. We start by describing the scaling model and then discuss the findings from the SCF calculations.

Results and Discussion

1. Scaling Model. As noted above, we assume that the copolymers in solution contain stickers that bind to specific sites on the surface. Each linear copolymer contains m uniformly distributed stickers. The chain contains a total of N monomers; thus, the concentration of stickers in each copolymer is given by $c = m/N$. All chains are assumed to be chemically identical. The concentration of chains in the solution is held constant, and μ denotes the chemical potential for a copolymer in the bulk fluid.

The heterogeneous substrate (or viral particle) is modeled as a planar interface, whose surface area is equal to Σ. This surface contains attractive binding sites, or receptors, that are located at a specific distance with respect to each other. When a sticker is bound to a receptor, the energy of the system is lowered by an amount ϵ, which corresponds to the difference in free energies between a sticker in solution and a sticker attached to the binding site. We assume that $\epsilon/kT \gg 1$, which corresponds to strong binding between the polymer and substrate.[10] Here and throughout the paper, k is Boltzmann's constant and T is temperature.

The "bare" surface, representing a red blood cell, is also modeled as a planar surface of area Σ. By bare, we mean that this surface does do not possess a protective polymer coating. One component of the interaction between the bare and coated surfaces (cells and the viral particles) is modeled by a van der Waals attraction. As is conventional for colloidal systems, we assume that the attractive part of the cell−virus interaction, ΔW, is governed by an effective Hamaker constant $A > 0$. Since we model the viral particles and the cells as two planar surfaces, each of area Σ, we have[11]

$$\Delta W = -A\Sigma/12\pi H^2 \qquad (1)$$

where H is the distance between the cell and virus.

The repulsive part of the cell−virus interaction is determined by the protective polymer layer. Due to the compression of the polymer coating, there is an increase in the local osmotic pressure, which tends to push the particles apart. This stabilizing force becomes noticeable when the distance H between the cell and the virus is less than the average thickness H_o of the polymer layer. Thus, to calculate the repulsive force, we must first determine the structure and thickness of the noncompressed polymer film that covers the viral particle.

(i) Undeformed Polymer Layer. We consider the equilibrium adsorption of copolymers onto a heterogeneous surface. A rigorous analytical solution of this problem for arbitrary number of stickers and various distributions of binding sites is rather intractable. Certain special cases have been considered in the literature.[12] In this investigation, we use a series of simplifying approximations that nonetheless allows us to obtain a degree of insight into the problem. As noted in the Introduction, we also employ a numerical SCF method to compliment and verify our scaling predictions. We start, however, by describing our simple scaling model, which is based on the following assumptions.

First, we assume that the size of a receptor is equal to the size of a monomer, a, and the receptors form a quenched, regular array on the surface. The distance between these receptors is equal to d. The total number of receptors on the surface is given by $n_o = \Sigma/d^2$.

Due to the large interaction energy between the stickers and receptors ($\epsilon/kT \gg 1$), we further assume that all the stickers within the adsorbed polymers are bound to the surface. In other words, each adsorbed polymer forms a sequence of $(m - 1)$ loops and one tail. This conformation is shown in Figure 2a.[13] We let n be the total number of the adsorbed chains on the surface; thus, the total number of occupied sites is equal to nm. The fraction of receptors that are covered by stickers is given by $\alpha = nm/n_o$, while the rest of the $(1 - \alpha)n_o$ receptors remain unoccupied by sticker sites. In the analysis below, we assume that $\alpha < 1$, i.e., the binding sites are not saturated with stickers. In this case, the adsorbed polymers have enough room to attach all of their stickers to the receptors and form a uniform assembly of loops. (In the opposite limit, $\alpha = 1$, the adsorbed chains will display a greater variety of conformations, forming both loops and tails of different sizes.)

Finally, we assume that the average density of grafted loops, $\sigma = nm/\Sigma = \alpha/d^2$, is above the overlap threshold. Thus, we are in the regime where the loops form a

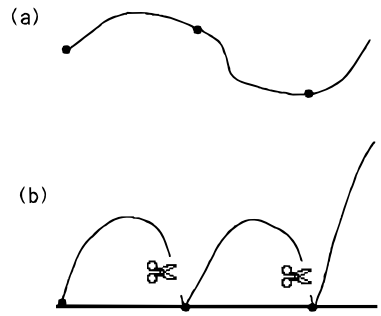

Figure 2. (a) Schematic drawing of the polymer containing m stickers. (b) Conformation of the tethered chain on the surface. In our scaling model, each loop is cut near one of the anchoring points. As a consequence, the loops are transformed into tails. Each tail is $N' = N/m$ units in length.

polymer brush. We can simplify the system even further by cutting each chain directly above one of its anchoring points, as shown in Figure 2b.[14] Now, the adsorbed layer consists of independent subchains (tails) of length $N' = N/m$, where each tail subtends an area equal to σ^{-1}.

The free energy (per unit area), ΔG, for such a system reads

$$\Delta G = \Delta E + \Delta F_{\text{brush}} + \Delta S \tag{2}$$

Here, ΔE is the change in the free energy (per unit area) due to the adsorption of stickers on the receptors

$$\Delta E = -\epsilon n m/\Sigma \tag{3}$$

The second contribution, ΔF_{brush}, describes the free energy of the subchains in the brush. We assume that the solution is a good solvent for the polymers. Then, ΔF_{brush} (per unit area) is given by[15a,b]

$$\Delta F_{\text{brush}}/kT = bN'\,(nm/\Sigma)(\sigma a^2)^{2/3} = ba^{4/3}N\rho^{5/3}\,m^{2/3} \tag{4}$$

where $\rho = n/\Sigma$ is the concentration of adsorbed chains on the surface and b is a numerical coefficient on the order of unity. The last contribution in eq 2 is the entropy of mixing for the free and the occupied receptors on the surface. This term is related to the number of possible ways in which the n indistinguishable sites can be occupied by the stickers. Since the subchains are now treated as independent elements, we adopt the following formulation for the entropy of mixing (per unit area) for the system

$$\begin{aligned}\Delta S/kT &= d^{-2}[\alpha \ln(\alpha) + (1-\alpha)\ln(1-\alpha)] \\ &= d^{-2}[(m\rho/\rho_o)\ln(m\rho/\rho_o) + \\ &\qquad (1 - m\rho/\rho_o)\ln(1 - m\rho/\rho_o)]\end{aligned} \tag{5}$$

where $\rho_o = 1/d^2$. The total free energy per unit area yields

$$\begin{aligned}\Delta G/kT = -\epsilon m\rho/kT + ba^{4/3}Nm^{2/3}(\rho)^{5/3} + \\ d^{-2}[(m\rho/\rho_o)\ln(m\rho/\rho_o) + (1 - m\rho/\rho_o)\ln(1 - m\rho/\rho_o)]\end{aligned} \tag{6}$$

The chemical potential of the adsorbed chains, $\mu_a = \delta(\Delta G\Sigma)/\delta n = \delta G/\delta\rho$, is given by

$$\begin{aligned}\mu_a/kT = -m\epsilon/kT + 5ba^{4/3}Nm^{2/3}\rho^{2/3}/3 + \\ m\ln[(m\rho/\rho_o)/(1 - m\rho/\rho_o)]\end{aligned} \tag{7}$$

By equating the chemical potential of the adsorbed chains to that of the chains in solution, $\mu_a = \mu$, we can rewrite eq 7 in the following way, which then yields the adsorption isotherm:

$$\begin{aligned}\mu/kT = -m\epsilon/kT + 5ba^{4/3}\,Nm^{2/3}\rho^{2/3}/3 + \\ m\ln[(m\rho/\rho_o)/(1 - m\rho/\rho_o)]\end{aligned} \tag{8}$$

Equation 8 relates the concentration of polymers on the surface, ρ, to the parameters of the system: the concentration of polymer in the bulk solution (or the value of μ), the molecular weight of the chains, N, the number of stickers, m, and the distance between the receptors, $d = \rho_o^{-1/2}$.

We now assume that the range of polymer concentrations in the bulk solution is such that the system is in the "plateau" regime of the adsorption isotherm, where the adsorbed amount is virtually independent of the bulk concentration of polymer. Here, the concentration of polymer on the surface, ρ, is predominantly determined through a balance of the adsorption energy (first term in the right side of eq 8) and the free energy of the brush (second term in the right side of eq 8). The contributions to ρ due to the mixing entropy and the bulk chemical potential are negligible. Thus, we can solve for ρ by equating the magnitude of the first and second terms in eq 8. From this calculation, we can then determine the adsorbed amount of polymer, θ

$$\theta = N\rho a^2 = (\epsilon/kT)^{3/2}c^{1/2} \tag{9}$$

where again $c = m/N$ is the concentration of stickers in a polymer chain. The area per subchain, $s = \sigma^{-1} = (m\rho)^{-1}$, is now given by

$$sa^{-2} = (\epsilon c/kT)^{-3/2} \tag{10}$$

The thickness of the brush,[15] $H_o = a(N/m)(sa^{-2})^{-1/3}$, can now be rewritten as

$$H_o = a(\epsilon/kT)^{1/2}c^{-1/2} \tag{11}$$

The corresponding value of the brush free energy, ΔF_{brush}, scales as

$$\Delta F_{\text{brush}}/kT = a^{-2}(\epsilon/kT)^{5/2}c^{3/2} \tag{12}$$

As indicated by eqs 9−12, the characteristics of the polymer coating depend solely on the binding energy of the sticker, ϵ, and the concentration of stickers within the polymer chain, c. In our model, we find that the characteristics of the film do not depend on the distance between the receptors. This is due to the fact that the d-dependent contribution to the free energy (the entropy of mixing term, which is the third term in eq 8) is relatively small in comparison to the other terms in this expression and was thus omitted in our calculation of θ (eq 9). Our finding implies that, within the plateau regime of the adsorption isotherm, the behavior is qualitatively similar for uniformly adsorbing surfaces and heterogeneous substrates (given the applicability of our model, see further below).

Our results indicate that increases in both the adsorption energy, ϵ, and the concentration of stickers, c,

lead to an increase in the adsorbed amount of polymer, θ, (see eq 9). The thickness H_o of the layer, however, decreases with increases in c. Despite an increase in θ and a corresponding decrease in s (see eq 10), the molecular weight of the subchains decreases linearly with increases in the concentration of stickers: $N' = N/m = c^{-1}$. This behavior leads to the overall decrease in H_o, the thickness of the polymer layer.

The above results are only valid in a certain region of parameter space. Namely, within the model, the formation of a brush by the subchains requires the equilibrium area per anchored chain, s, to be lower than the overlap threshold. In other words, the area per chain should be less than the radius of gyration of the subchain, which is of length (N/m) and assumed to be in a good solvent. This implies that $s < (N/m)^{6/5}a^2$. By applying eq 10, we find the latter condition imposes a limitation on the concentration of stickers. In particular, the sticker concentration is limited from below in the following way:

$$c > (\epsilon/kT)^{-5} \tag{13}$$

Since $\epsilon/kT \gg 1$, this is not a crucial restriction.

We can also check that our neglect of the entropy of mixing term in eq 8 is justified when $\alpha = m\rho/\rho_o \ll 1$. By ignoring the logarithmic dependence on α in the third term of eq 8 and using eq 9, we find that mixing entropy is indeed negligible with respect to the brush free energy when $\epsilon/kT \gg 1$. However, the restriction $\alpha < 1$ imposes a limitation on the range of values for c. Namely, eq 9 indicates that c should be limited from above in the following way

$$c < (\epsilon/kT)^{-1}(d/a)^{-4/3} \tag{14}$$

in order to prevent the saturation of the surface by adsorbed polymer ($\alpha = 1$). In our analysis below, we assume both inequalities (13) and (14) are satisfied, and we move on to consider the protective properties of the polymer coatings.

(ii) Stabilization of the Cells. We can now analyze the repulsive interaction between the bare and polymer-coated surface (between the cell and coated virus). As mentioned above, compression of the protective layer induces a repulsive osmotic force, which pushes the particles apart. We assume that compression of the polymers does not lead to their desorption, and thus the adsorbed amount, θ (and the area per chain s), remains constant during the compression. We adopt the simple Alexander−de Gennes model[16,17] to determine the increase in the free energy of the system due to compression of the layer. Namely, we write the repulsive (polymer) contribution to the interaction between the particles as[18]

$$\Delta F(H) = \Delta F_{brush}\Sigma\{(1/3)(H/H_o)^2 + (2/3)(H_o/H) - 1\} \tag{15}$$

where $H < H_o$ is the distance between the particles and H_o and ΔF_{brush} are given by eqs 11 and 12, respectively. The first term in the brackets in eq 15 describes the relaxation in the stretching of the chains due to compression, and the second term describes an increase in the repulsive interactions between polymer units, while the last term provides a reference state ($\Delta F(H_o) = 0$). The above expression for ΔF is based on a mean field approximation for the interactions between the polymers and corresponds to good solvent conditions.

The total interaction between the colloidal particles then yields

$$\Delta U = \Delta W + \Delta F = -[A\Sigma/12\pi H_o^2](H_o/H)^2 + \Delta F_{brush}\Sigma\{(1/3)(H/H_o)^2 + (2/3)(H_o/H) - 1\} \tag{16}$$

Our goal is to analyze the shape of the total interaction curve, $\Delta U(H)$, and delineate its extrema. By differentiating $\Delta U(H)$ with respect to H and introducing the reduced distance $y = H/H_o < 1$, we arrive at the following equation

$$B(y^4 - y) + 1 = 0 \tag{17}$$

where the parameter $B = 4\pi\ \Delta F_{brush}H_o^2/A$. Recalling that $|\Delta W_o| = A\Sigma/12\pi H_o^2$ (eq 1), we can solve for A and insert the result into the expression for B. This yields $B = \Sigma\Delta F_{brush}/(3|\Delta W_o|)$, and hence, the parameter B is a ratio of the brush free energy, $\Delta F_{brush}\Sigma$, and the van der Waals attractive energy for particles separated a distance H_o. By analysis of eq 17, it can be seen that the equation only has solutions if B exceeds a certain critical value, B^*, which is on the order of unity ($B^* \cong 1$). In physical or scaling terms, this means that the polymer coating can only provide steric stabilization when the free energy of the brush, $\Delta F_{brush}\Sigma$, is comparable to or larger than $|\Delta W_o|$. In the opposite case, the van der Waals attraction between the particles is too strong, and this attraction leads to the coagulation of the particles.

At $B \gg B^* = 1$, the solutions of eq 17 can be approximated as $y_1 = 1/B$ and $y_2 = 1 - 1/(3B)$. The first solution corresponds to a maximum in the interaction curve $\Delta U(H)$ that is located at $H = H_{max} = H_o/B \ll H_o$. The value of the maximum, $\Delta U_{max} = \Delta U(H_{max})$, can be evaluated from eq 16 as

$$\Delta U_{max} = \Sigma\Delta F_{brush}B/3 = (\Sigma\Delta F_{brush})^2/(9|\Delta W_o|) \tag{18}$$

The second solution corresponds to a minimum located at $H = H_{min} = H_o[1 - 1/(3B)] \approx H_o$. The value of $\Delta U_{min} = \Delta U(H_{min})$ can be estimated from eq 16 as

$$\Delta U_{min} = \Delta W_o \tag{19}$$

Figure 3 schematically illustrates the shape of the interaction curve, ΔU(H), between the bare and covered surfaces (a cell and virus), as determined by eq 16. It indicates that the curve exhibits a maximum, which is separated by the two minima. The first minima is located at infinitely small distances between the particles, $H = 0$ (the so-called primary minimum), and the second one is located at $H = H_o$ (the so-called secondary minimum). Depending on the relative depth of the secondary minimum, ΔU_{min}, and the height of the maximum, ΔU_{max}, the colloidal system will exhibit different behavior. Namely, when the height of the maximum is small relative to the thermal energy of the particles, i.e., $\Delta U_{max} \ll kT$, the particles will overcome the barrier and coagulate in the primary minimum. When the height of the barrier is large enough, i.e., $\Delta U_{max} \gg kT$, the particles are prevented from coagulation in the primary minimum. However, if the depth of the secondary minimum is comparable to kT, the particles can aggregate in the secondary minimum, and the dispersion will still be thermodynamically unstable.

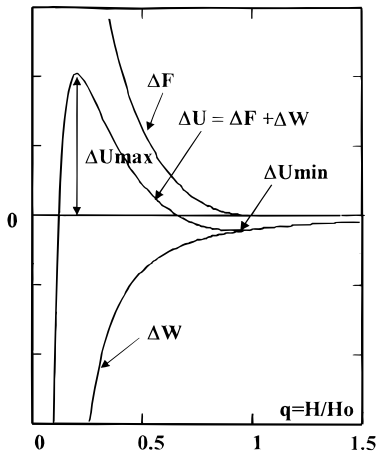

Figure 3. Schematic plot for the interaction curve, $\Delta U(H)$, between the bare and covered surfaces. The curve exhibits a maximum, which is separated by the two minima. The primary minimum is located at infinitely small distances between the particles and the secondary minimum is located at a distance that is essentially the height of the polymeric layer, H_o.

A stable dispersion of particles is formed only when the following two conditions are fulfilled:

$$\Delta U_{max} \gg kT \qquad |\Delta U_{min}| \ll kT \tag{20}$$

In other words, when these conditions are met, the cells and virus will not aggregate, but will be pushed apart due to the protective polymer coating.

In our scaling model, the necessary conditions for the stability of the dispersion can be formulated in terms of the molecular parameters, c and ϵ, by employing eqs 11, 12, and 18−20. Specifically, we find that the stability range for our dispersion is determined by the inequality

$$(\Sigma/a^2)^{-1/2}\,(A'/kT)^{1/2}\,(\epsilon/kT)^{-3} = c_1 < c < c_2 = (\epsilon/kT)(\Sigma/a^2)^{-1}(A'/kT)^{-1} \tag{21}$$

where $A' = A/(12\pi)$ and all the other numerical coefficients that are on the order of unity have been omitted.

Our findings indicate that there is an intermediate range of sticker concentrations that sterically stabilize the solution and thus, inhibit contact between the cells and virus. At the lower boundary in eq 21, $c = c_1$, the barrier in the $\Delta U(H)$ interaction curve goes below kT. Correspondingly, at $c < c_1$, the polymer coating on the viral particle becomes too loose to prevent aggregation of the virus and the cell, and the particles aggregate in the primary minimum. At the upper boundary, $c = c_2$, the attractive secondary minimum in the $\Delta U(H)$ curve becomes deeper than kT. As a result, at $c > c_2$, the polymer layer is too thin to prevent the virus from approaching the cell. Although the coating now contains more polymer chains and provides stronger repulsion upon compression, the virus approaches the cell up to the distance H_o without "feeling" the presence of polymer. Even if it is then stopped by polymer (at $H < H_o$), the attractive van der Waals energy between the cell and the virus, $|\Delta W_o| > kT$, is sufficiently large to bind these species together. As a result, cells and viruses will form aggregates that can contain many particles of both types. Thus, one expects that the optimal composition, c^*, for polymer chains lies between the two boundaries, c_1 and c_2, and the stability range passes through a maximum as c increases from c_1 to c_2.

The results reveal that the range of stability for the cell−virus dispersion can be affected by varying the interaction energy ϵ, the effective Hamaker constant A, and the surface area of the particle Σ. While the size of the viral particle is fixed, changing the chemical identity of the monomers in the chain can result in a change in A. Variations in ϵ can be obtained by changing the type of stickers or by decreasing the solvent quality (using mixed solvents).[19] In the latter case, one expects an increase in ϵ and the corresponding increase in the stability range, in the manner given by eq 21.

We recall, however, that the scaling model derived in this section is rather approximate and only gives a general picture of the cell−virus interactions. To obtain further insight into the problem, we use the SCF method described below; these calculations yield a more detailed picture of the protective properties of "'sticky" polymers.

2. Self-Consistent Field Model. Our self-consistent field (SCF) calculations are based on the model developed by Scheutjens and Fleer.[20] In the Scheutjens and Fleer theory, the phase behavior of polymer systems is modeled by combining Markov chain statistics with a mean field approximation. Since the method is thoroughly described in ref 20, we simply provide the basic equations and refer the reader to that text for a more detailed discussion.

These calculations involve a planar lattice where one lattice spacing represents the length of a statistical segment within a polymer chain. The planar lattice is divided into $z = 1-M$ layers. In the one-dimensional model, the properties of the system only depend on z, the direction perpendicular to the interface. The properties of the system are averaged over the x and y directions; that is, the system is assumed to be translationally invariant in the lateral direction. The probability that a monomer of type i is in layer z with respect to the bulk is given by the factor

$$G_i(z) = \exp(-u_i(z)/kT) \tag{22}$$

where the potential $u_i(z)$ for a segment of type i in layer z is given by

$$u_i(z) = u'(z) + kT\Sigma_{j(\neq i)}\,\chi_{ij}\,(\langle\phi_j(z)\rangle - \phi_j^{\,b}) \tag{23}$$

The parameter $u'(z)$ is a "hard-core potential", which ensures that every lattice layer is filled. In the second term, χ_{ij} is the Flory−Huggins interaction energy between units i and j and $\phi_j^{\,b}$ is the polymer concentration in the bulk. The expression $\langle\phi_j(z)\rangle$ is the fraction of contacts an i segment in the z layer makes with j-type segments in the adjacent layers and is given by the following equation:

$$\langle\phi_j(z)\rangle = \lambda_{-1}\phi_j(z-1) + \lambda_0\phi_j(z) + \lambda_1\phi_j(z+1) \tag{24}$$

Here, the λ's are the fraction of neighbors in the adjacent layers: λ_{-1} is for the previous layer, λ_0 is for the same layer, and λ_1 is for the next layer.

Since polymers contain more than one segment, we must take into account that the segments of the chain are connected. We define $G_i(z,s|1)$ as the (conditional) probability (up to a normalization constant) that a segment s is located in layer z, while being connected to the first segment of chain i. This Green's function

can be calculated from the following recurrence relation:

$$G_i(z,s|1) = G_i(z)\{\lambda_{-1}G_i(z-1,s-1|1) + \lambda_0 G_i(z,s-1|1) + \lambda_1 G_i(z+1,s-1|1)\} \quad (25)$$

Clearly, $G_i(z,1|1) = G_i(z)$ and the terms for $s > 1$ can be calculated from this relationship and eq 25. In the same way, we can obtain a recurrence formula for $G_i(z,s|r)$, the probability that a segment s is in layer z, given it is connected to the last (rth) segment of the chain.

To obtain the volume fraction of i in the z layer due to segment s, in a chain of r segments, the product of two probability functions is needed: the probability of a chain starting at segment 1 and ending with segment s in layer z and that of a chain starting at segment r and also ending with segment s in layer z. This product must be divided by $G_i(z)$ in order to compensate for the double counting of the sth segment. Hence, the volume fraction is given by

$$\phi_i(z,s) = C_i G_i(z,s|1)G_i(z,s|r)/G_i(z) \quad (26)$$

Here, C_i is the normalization constant and is equal to $C_i = \theta_i/r_i\Sigma_z G_i(z,r|1)$ where $\theta_i = \Sigma_z\phi_i(z)$ is the total amount of polymer segments of type i in the system and $\Sigma_z G_i(z,r|1)/M$ is the average of the end segment distribution function for a chain of r_i segments. We can also express C_i in terms of ϕ_i^b, the volume fraction in the bulk solution, as $C_i = \phi_i^b/r_i$. The total volume fraction of $\phi_i(z)$ of molecules i in layer z can be obtained by summing over s:

$$\phi_i(z) = \Sigma_s\phi_i(z,s) \quad (27)$$

Expressions 22 and 26, and the condition that $\Sigma_i\phi_i(z) = 1$ for each layer, form a set of coupled equations that are solved numerically and self-consistently. Given that the amount of polymer, θ_i, the length r_i, and χ_{ij} are specified, we can calculate the self-consistent adsorption profile and the equilibrium bulk concentration. (For a given θ_i, ϕ_i^b is obtained by equating the two expressions for C_i.) We also calculate the amount of copolymer adsorbed at the surface, Θ_{ex}, which is given by

$$\Theta_{ex} = \Sigma_z(\phi(z) - \phi^b) \quad (28)$$

Here, $\phi(z)$ is the concentration of polymer in layer z, and the sum is over all lattice layers.

We note that the expression for the excess free energy in terms of the segment density distribution is given by

$$F(z) = \Sigma_j\phi_j(z)\ln G_j(z) + (1/2)\Sigma_{jk}\chi_{j,k}\int \eta(z-z')\phi_j(z)\phi_k(z')\,dz' \quad (29)$$

Summing the above equation over all z yields the total free energy (per unit area). The free energy of interaction between two surfaces, ΔF_{int}, as a function of surface separation, H, can be obtained by taking the difference between the total free energies when the layers are infinitely apart and when they are separated by a distance H. (We emphasize that ΔF_{int} is a free energy per unit area. Thus, we must multiply this value by the area of the surface to obtain a free energy.)

To examine systems that contain lateral heterogeneities on the surface, such as distinct binding sites, we must resort to the two-dimensional SCF theory,[21] where the above equations are explicitly written in terms of z and y, directions perpendicular and parallel to the surface. In the two-dimensional version, we nonetheless assume translational invariance along x. Carrying out a full three-dimensional calculation, which would more accurately capture the features of the actual surface, is computationally prohibitive. Thus, we are forced to consider more simplified models of the surface, which nonetheless capture the effect of the heterogeneities. To this end, we performed two different types of calculations, which we refer to as the "square lattice" and "cubic lattice" calculations.

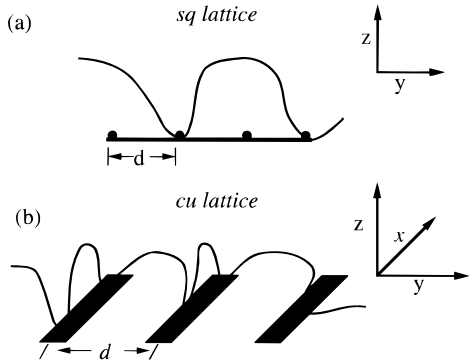

Figure 4. (a) The receptors in the *sq* lattice line along a line and are located a distance d from each other. To emphasize the location of these sites, they are marked by dark circles. The chains are localized in a two-dimensional square lattice. (b) The receptors in the *cu* lattice are modeled by parallel stripes (or lines) separated by a distance d. (For emphasis, the stripes are drawn multiple sites thick.) The chains occupy a three-dimensional cubic lattice.

The square lattice calculation (or "*sq*") implies that our system is two-dimensional. Here, the heterogeneous substrate is modeled as an impermeable line, while the polymer chains are generated on a planar square lattice (where the coordination number of the lattice is $q = 4$). The receptors are modeled by adsorbing sites on the line; the sites are located a distance d from each other. The cubic lattice calculations (or "*cu*") involve a planar (two-dimensional) substrate and the chains are generated in a three-dimensional cubic lattice ($q = 6$). The receptors, however, are modeled by parallel stripes (or lines) separated by a distance d. Thus, in the *sq* calculations we underestimate the set of conformations that are accessible to the adsorbing polymers, but we capture the discrete nature of the receptors. In the *cu* calculations, we treat the polymers properly, but account for the discreteness of the receptors in an approximate manner. Namely, the receptors (stripes) are discrete in the y direction, but are continuous in the x direction (see Figure 4). Thus, the polymer can adsorb onto a single receptor multiple times before, or instead of, passing onto an adjacent binding site. (As we note below, at low sticker concentrations, the polymers actually exhibit a high degree of bridging between adjacent receptors.) We use both types of data in our analysis.

(i) Copolymer Adsorption on the Surface. We start with an analysis of the adsorption of the copolymers onto the heterogeneous substrates. Figure 5 shows the excess adsorbed amount, Θ_{ex}, vs sticker concentration, c, for both the *cu* (Figure 5a) and *sq* (Figure 5b) calculations. The curves are for various distributions of receptors on the surface. The specific arrangement of the receptors is described by two

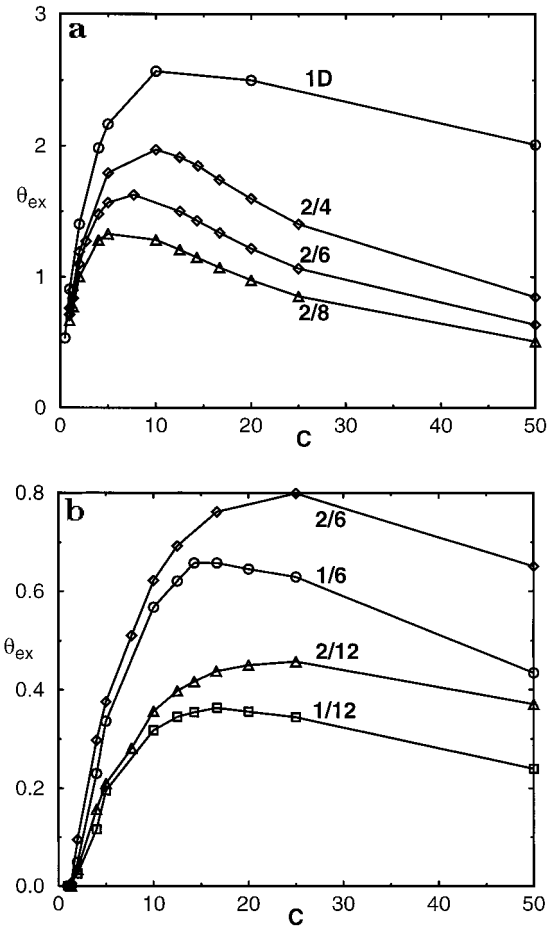

Figure 5. Excess adsorbed amount per unit area, Θ_{ex}, vs c, the sticker concentration. The chain length is fixed to $N = 2000$. (a) Calculations for the *cu* lattice. Here, $\epsilon/kT = 17$. The curve labeled 1D refers to calculations for a homogeneous, adsorbing surface, where the stickers are uniformly attracted to all the surface sites. (b) Calculations for the *sq* lattice. Here, $\epsilon/kT = 7.5$. The numbers on the curves describe the arrangement of the receptors on the surface: the first number indicates the width of each receptor (the number of contiguous lattice sites), and the second number is the distance between neighboring receptors.

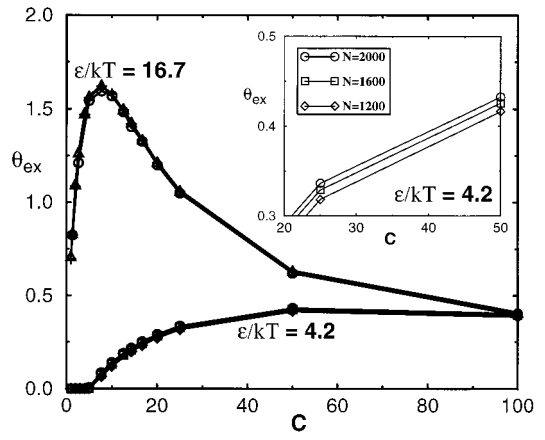

Figure 6. The excess adsorbed amount per unit area, Θ_{ex}, vs c, the sticker concentration, for various chain lengths, N. The results are for the *cu* calculations at two different adsorption energies, $\epsilon/kT = 17$ and $\epsilon/kT = 4$. Since the curves for various N cannot be readily distinguished on the central plot, the inset shows a blowup of the curves for $\epsilon/kT = 4$ and low sticker concentrations.

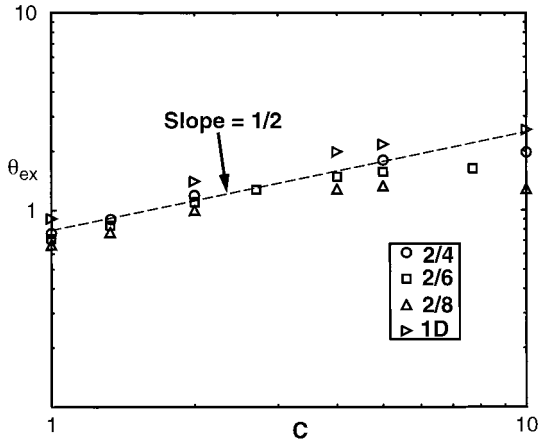

Figure 7. A log−log plot of the excess adsorbed amount per unit area, Θ_{ex}, vs sticker concentration, c. The results are from the *cu* calculations. The dashed line serves as a guide to the eye and marks a slope of $^1/_2$.

numbers: the first number indicates the width of each receptor (the number of contiguous lattice sites), and the second number is the distance between neighboring receptors. In both the *cu* and *sq* cases, Θ_{ex} is a nonmonotonic function of c and exhibits a maximum at relatively low concentrations of stickers. As indicated by parts a and b of Figure 5, increasing the distance d between the receptors leads to a decrease in the amount of adsorbed polymer. The maximum adsorbed amount is obtained for a uniformly adsorbing substrate.

In the range of low sticker concentrations (to the left of the maximum), the curves corresponding to different d's effectively collapse onto a single master curve. It is for this range of parameters that our scaling model is expected to be most valid.

Figure 6 displays Θ_{ex} vs c for various values of N, the molecular weight of the chains. Since the plots for the different N all lie atop each other, the figure indicates that the relationship between Θ_{ex} and c is independent of N. These data from the SCF calculations agrees with the scaling prediction for Θ_{ex} in eq 9. The specific dependence of Θ_{ex} on the concentration of stickers can be obtained from the log−log plot in Figure 7. Again, the data are in good agreement with the scaling prediction in eq 9. In particular, the dashed line has a slope of $^1/_2$, and the data show only slight deviations from the theoretically predicted slope.

The SCF results for the dependence of Θ_{ex} on the sticker−receptor interaction, χ_{sr}, also reveal reasonable agreement with the scaling model. Specifically, the slope of $\log(\Theta_{ex})$ vs $\log(\chi_{sr})$ is close to the theoretical prediction of $^3/_2$ given by eq 9. Note that to relate the Flory−Huggins parameter χ_{sr} to ϵ/kT and, thus, experimentally relevant values, we must divide χ_{sr} by the coordination number of the lattice, q. In other words, $\epsilon/kT = -\chi_{sr}/q$. This relationship can be explained as follows. Consider the sticker to be a cube in our lattice model. When a sticker attaches to the substrate and gains an adsorption energy ϵ/kT, the sticker only contacts the surface through one face of the cube. The other $(q - 1)$ faces are still in contact with the solvent. As a result, the free energy of an adsorbed sticker is changed with respect to its state in the solution by a factor $(\chi_{sr} - \chi_{ps})/q$, where χ_{ps} is the Flory−Huggins parameter for the polymer−solvent interaction. By definition, $(-\epsilon/kT)$ is the difference in the sticker free energy on the substrate and in solution; hence, $-\epsilon/kT = (\chi_{sr} - \chi_{ps})/q$. Since we focus on the case of a good solvent, $\chi_{ps} = 0$, and thus, $\epsilon/kT = -\chi_{sr}/q$.

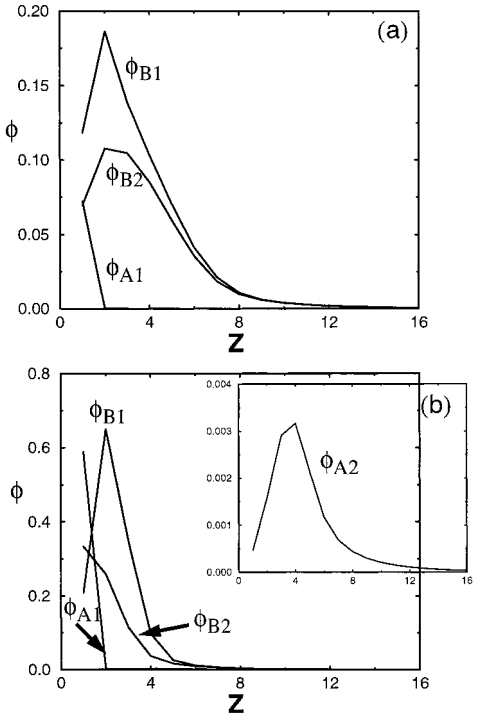

Figure 8. Polymer density profiles for the adsorbed layer. The *z*-direction lies perpendicular to the surface.The plots are obtained from *cu* calculations with $N = 2000$ and $\epsilon/kT = 12.5$. In part a, $c = 2\%$. The profile for ϕ_{A2} is too small to be detectable on this plot. In part b, $c = 10\%$. The profile for ϕ_{A2} has been blown up in the inset. Note that the polymer layer is significantly thinner for the higher sticker concentration.

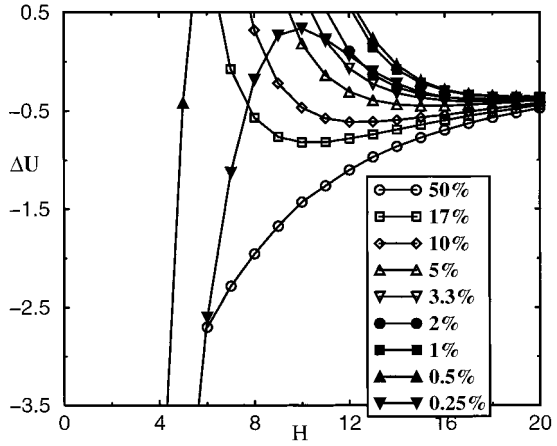

Figure 9. Interaction curves: the total free energy, ΔU, vs H, for various sticker concentrations, c. Here, $\epsilon/kT = 12.5$, $A/12\pi kT = 0.02$, and $d = 6$. Unless stated otherwise, the receptors are taken to be one lattice site in width. The results are from the *cu* calculations.

As the concentration of stickers in the chain increases, the curves $\Theta_{ex}(c)$ corresponding to different values of d begin to diverge. The maximum of the curves is shifted to lower values of c as the distance d between receptors is increased. To the right of the maximum, the effect of the discrete nature of the adsorbing sites is quite pronounced. To the left of the maximum, however, the deviations from the master curve caused by changes in d are relatively small. Within this range, the effect of increasing d can be ascertained by considering the full expression for the adsorption isotherm, eq 8. As indicated by this equation, increases in $d = (\rho_o)^{-1/2}$ lead to an increase in the mixing entropy term (last term on the right side of eq 8). Since the chemical potential of the adsorbed chains is fixed (and is equal to the chemical potential of the free chains, μ), an increase in the mixing entropy term is balanced by a decrease in the "brush" contribution (second term on the right side of eq 8). The decrease in the brush term is, in turn, brought about through a decrease in ρ, the concentration of polymers on the surface. Thus, at low concentration of stickers, eq 8 indicates a slight decrease in ρ due to increases in d.

Figure 8 shows the typical distribution of polymer units in the adsorbed layer. Here, z is the distance normal to the substrate. We plot the density profile for the stickers (a) and the profile of nonadsorbing units (b). The stickers are primarily localized on the receptors, while the nonadsorbing units form a diffuse polymer layer above the surface. To further investigate the pattern of adsorption onto the laterally inhomogeneous substrate, we examine the "partial" profiles, $\phi_{A1}(z)$, $\phi_{A2}(z)$, $\phi_{B1}(z)$, and $\phi_{B2}(z)$. The profile $\phi_{A1}(z)$ indicates the total fraction of stickers located at distance z above the receptors within the substrate. The profile $\phi_{A2}(z)$ indicates the fraction of stickers above the nonadsorbing part of the surface, so that the sum of the two terms, $\phi_{A1}(z) + \phi_{A2}(z)$, gives the total fraction $\phi_A(z)$ of A units at a distance z from the substrate. The same definitions hold for the B units. Namely, $\phi_{B1}(z)$ is the fraction of B units located above the receptors on the substrate, and $\phi_{B2}(z)$ refers to the B units above the nonadsorbing part of the surface. The total profile for the B units, $\phi_B(z)$, is given by $\phi_{B1}(z) + \phi_{B2}(z)$. The above profiles allow us to monitor the frequency of "transitions" from receptor to receptor. This is particularly important for the *cu* calculations, where the polymer can form long sequences of loops along a single adsorbing line. For low concentrations of stickers, we examine the fraction of B's above the binding and nonbinding sites. If the distribution of B's is relatively uniform, we can conclude that the chains form bridges between different receptors. When performing the *cu* calculations, we check that the receptor-to receptor transitions do indeed take place.

(ii) Interactions between Polymer-Coated and Bare Surfaces. We now analyze the interactions between a substrate covered with adsorbed polymers (the viral particle) and the bare surface (the cell). As mentioned above, we assume that the amount of adsorbed polymer, Θ_{ex}, remains constant as the two surfaces come in close contact. (The SCF calculations do in fact show that for all but very low sticker concentrations, Θ_{ex} only decreases a few percent when the layer is compressed.) Keeping Θ_{ex} fixed, we calculated the free energy of the system at various distances between the surfaces. This part of the free energy constitutes the repulsive contribution, which arises from the deformation of the polymer layer. By adding the attractive part, which is due to the van der Waals forces between the particles (eq 1), we obtain the total interaction curve.

In the first set of calculations, we fixed the relevant parameters at the following values: $N = 2000$, $A/12\pi kT = 0.02$, the concentration of polymer in solution, $\phi_b = 10^{-10}$, the distance between the receptors, $d/a = 6$, and $\Sigma/a^2 = 10^4$. (We note that in this lattice model, the distance between two adjacent lattice sites (a lattice bond), and is comparable to 1 nm.) The corresponding curves of the total free energy, ΔU, vs H for various stickers concentrations are shown in Figure 9 for the *cu* lattice. In the subsequent set of calculations, we

varied the values of the Hamaker constant, the adsorption energy of the sticker, and the distance between the receptors. Through these investigations, we can assess how changes in the nature of the polymer or the surface affect the interaction between the particles.

As seen from Figure 9, the interaction curves have different shapes at different values of c. Namely, $\Delta U(H)$ can monotonically decrease, exhibit a minimum (as in the majority of the curves in the figures), and, in some cases, demonstrate a maximum. We recall that our scaling model predicts the existence of a maximum in the $\Delta U(H)$ curve for colloidal interactions involving a polymer-coated particle. (This maximum is followed by the primary minimum at smaller surface separations.) Our scaling model does not, however, account for higher-order interactions that can occur when the polymer is compressed. A more rigorous analysis based on both the Flory−Huggins model for polymer solutions and the numerical SCF model indicates that the primary minimum can be canceled due to ternary and the higher order contacts. This is why we do not find a maximum in all the SCF interaction curves, but instead find an increase in the free energy $\Delta U(H)$, even up to the point where the polymer layer is densely packed. This effect, however, does not change the major conclusions of our scaling model. Namely, to have a stable dispersion, there should be a shallow secondary minimum at distances where the coated and bare particles come into contact and a high maximum (or monotonic increase in ΔU) at small separations between the particles. To establish a criterion for isolating the cases where the dispersion is stable, we specify that the value of the secondary minimum, ΔU_{min}, must be $\geq -1kT$.

Figure 9 indicates that increases in c dramatically alter the interaction curve between the particles. This figure presents the data from *cu* calculations that were performed for $\epsilon/kT = 12.5$. At very low sticker concentrations, the adsorbed amount is insufficient to provide proper repulsion between the particles. Here, the maximum is either absent or is very low (as for $c =$ 0.25%) and the particles aggregate in the primary minimum. Increases in c lead to a rapid rising of the maximum. At $c = 0.5\%$, the maximum is already sufficient to prevent aggregation in the primary minimum. The depth of the secondary minimum is also less than $1kT$ and we can delineate $c = 0.5\%$ as the lower boundary of the stability range (equivalent to c_1 in our scaling model). Increases in c lead to further improvement in the stabilizing properties of the polymer at strong compression (close contact). Beyond 17%, however, increases in c are accompanied by a shift and deepening of the secondary minimum. The development of such a secondary minimum is due to the shrinking of the protective polymer coating. Indeed, in accordance with eq 11, the thickness of the adsorbed layer H_o decreases with increases in c. As a result, the secondary minimum is shifted to smaller values of H and becomes deeper. At $c = 17\%$, the depth of the secondary minimum is already around $1kT$, and the particles now start to aggregate in the secondary minimum. We can thus delineate $c = 17\%$ as an upper boundary, c_2, of the stability range. At higher values of c (see curve for $c =$ 50%) the dispersion is unstable.

A comparison of Figures 9 and 10 reveals the role of the Hamaker constant in the stability of the dispersion. (Varying A is comparable to changing the chemistry of the monomers within the chain.) The interaction curves

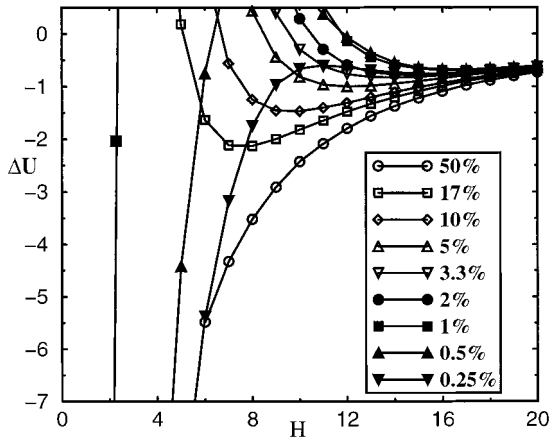

Figure 10. Interaction curves, ΔU vs H, for various sticker concentrations, c. Here, $\epsilon/kT = 12.5$, $A/12\pi kT = 0.03$, and $d =$ 6. The results are from the *cu* calculations.

in Figure 10 were calculated for the same parameters as in Figure 9, except the value of $A/12\pi kT$ was increased to 0.03. An increase in A corresponds to an increase in the attractive interaction between the particles. As can be seen from Figure 10, this increase results in a decrease in the range of sticker concentrations that yield a stable dispersion. Recall that our scaling model predicts that $c_1 = A^{1/2}$ increases, while $c_2 = A^{-1}$ decreases when A is increased (see eq 21). Due to the rather limited range of A values that we examined in our SCF calculations, we are not able to verify the specific values of the exponents; nonetheless, a comparison of the interaction curves in Figures 9 and 10 confirms the trend predicted by the scaling theory. Indeed, while the interaction curve corresponding to $c =$ 0.25% still exhibits a maximum, the value of the maximum is shifted downward relative to the case in Figure 9. Thus, the lower boundary, c_1, is slightly shifted to higher concentrations of stickers. The shift is much more pronounced for the upper boundary, c_2. (Our scaling model also predicts a stronger A dependence for c_2 than for c_1.) By comparing the interactions curves in Figures 9 and 10 for $c = 10\%$ and 17%, we see that sticker concentrations that yield stable systems at $A/12\pi kT = 0.02$, give rise to unstable dispersions at $A/12\pi kT = 0.03$. (The depth of the secondary minimum for these values of c is now below $1kT$.) Thus, the upper boundary c_2 decreased rather noticeably with an increase in A (going from approximately 17% to 5%).

We note that decreasing $A/12\pi kT$ has an effect opposite to that seen in Figure 10. Decreasing A corresponds to decreasing the relative attraction between the surfaces. For $A/12\pi kT = 0.01$, the $\Delta U(H)$ curves in fact show a broader range of sticker concentrations that will stabilize the dispersion. In particular, c_1 is decreased to 0.25%, and c_2 is increased to at least 50%.

The trends seen in Figure 10 are mirrored in Figure 11, where we present the *sq* calculations. Here, the value of χ_{sr} ($= -50$) is adjusted to account for the difference in the coordination numbers of the *sq* and *cu* lattices and yet maintain $\epsilon/kT = 12.5$ in both calculations. The other parameters are the same as those for Figure 10. By comparing Figures 10 and 11, we find little difference in the results for the *sq* and *cu* calculations.[22] More precisely, we find essentially the same range of stability for our dispersion (the same values of c_1 and c_2) in both types of calculations. Comparisons

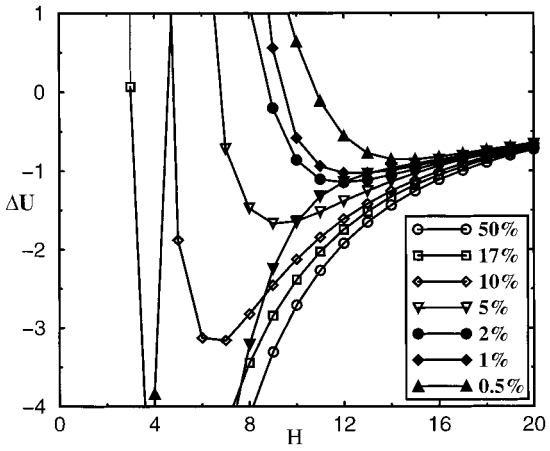

Figure 11. Interaction curves, ΔU vs H, for various sticker concentrations, c. Here, $\epsilon/kT = 12.5$, $A/12\pi kT = 0.03$, and $d = 6$. The results are from the *sq* calculations.

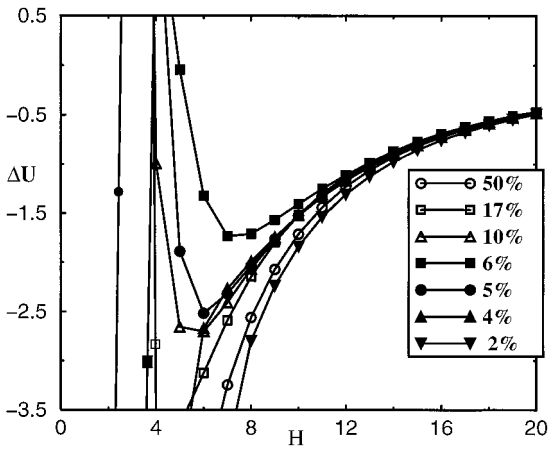

Figure 12. Interaction curves, ΔU vs H, for various sticker concentrations, c. Here, $\epsilon/kT = 7.5$, $A/12\pi kT = 0.02$, and $d = 6$. The results are from the *sq* calculations.

at $A/12\pi kT = 0.03$ and 0.01 also show remarkable similarly in the $\Delta U(H)$ curves for the *sq* and *cu* calculations. Thus, the results are not very sensitive to the specific lattice (*sq* vs *cu*) we use in these SCF studies.

Since the *sq* and *cu* calculations show similar trends, we focus mainly on the results of the *sq* calculations in the following discussion. Figure 12 serves to illustrate the effect of χ_{sr}, the sticker−receptor interaction energy, on the stability of the dispersion. Here, $A/12\pi kT = 0.02$ and $\chi_{sr} = -30$, which corresponds to $\epsilon/kT = 7.5$; all other parameters are the same as in Figures 9−11. By comparing the data in Figures 9 and 12, we see that decreasing ϵ has a significant effect on the system. Namely, all the curves now indicate that the dispersion is unstable, with the particles aggregating at the location of the secondary minimum. This behavior is in agreement with the scaling predictions. According to eq 21, decreases in ϵ lead to a rapid shrinking of the stability range. That is, $c_1 = (\epsilon/kT)^{-3}$ and $c_2 = (\epsilon/kT)$ rapidly approach each other as ϵ is decreased. Such a dramatic decrease in the stabilizing properties of the sticky polymers is due to the significant decrease in the amount of polymer adsorbed on the surface. (Through eq 9 in our scaling model, $\Theta_{ex} = (\epsilon/kT)^{3/2}$). The scf data in Figure 13 indicates a more than 2-fold decrease in Θ_{ex} as χ_{sr} is changed from $\chi_{sr} = -50$ to $\chi_{sr} = -30$ (or equivalently, as ϵ/kT is changed from 12.5 to 7.5).

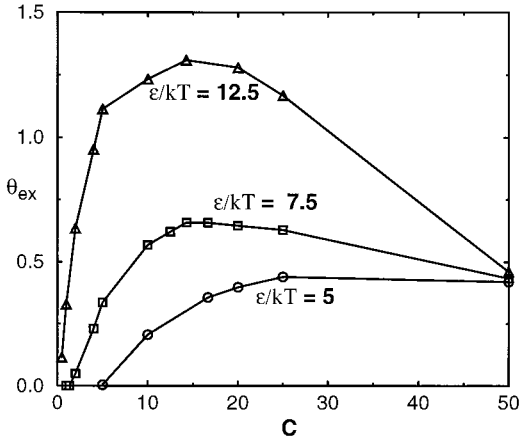

Figure 13. Excess adsorbed amount per unit area, Θ_{ex}, vs sticker concentration, c, for various adsorption energies for the *sq* calculations with $N = 2000$.

Finally, we investigate the effect of the "patchiness" of the substrate on the stability of the system. Figure 14a shows the interaction curves $\Delta U(H)$ when the size of a single patch or receptor is set at one lattice site and the distance between neighboring receptors is $d = 6$. For the chosen parameters ($A/12\pi kT = 0.01$ and $\epsilon/kT = 7.5$), the dispersion was stable for a wide range of sticker concentrations. Figure 14b depicts the changes in the interaction curves due to an increase in the receptor size from one to two sites, while the distance between the receptors is kept fixed ($d = 6$). Actually, we do not find many changes in the interaction curves, and the dispersion remains stable for a wide range of c. However, when the distance d between the receptors is increased 2-fold (and now equals 12, as in Figure 14c), the range of stability shrinks dramatically. Though the adsorption energies in cases a and c are equal, all the curves that pointed to the stability of the dispersion in Figure 14a, now indicate destabilization of the system in Figure 14c. These results highlight the subtle effect that the "patchiness" of the surface has on the interaction between the colloidal particles.

Conclusions

Using scaling theory and SCF calculations, we investigated the adsorption of sticker-containing copolymers onto laterally heterogeneous surfaces. (We note that our predictions on the structure of the adsorbed layer as a function of sticker concentration agree with our earlier studies, where we used Monte Carlo simulations to model the adsorption of copolymers onto a patterned sphere, which represented the influenza virus.[23]) We then correlated the sticker concentration with the ability of the adsorbed chains to sterically stabilize a dispersion of colloidal particles. Our results show a bell-shaped dependence between sticker concentration and the stability of the dispersion. Thus, chains containing too few stickers are as ineffective as those containing too many stickers. These findings are in agreement with experimental studies on the interactions between copolymer-coated influenza viruses and red blood cells. The inhibition between cell and virus contact shows a similar bell-shaped dependence on the concentration of sialic acid groups (stickers) in the adsorbing copolymers. Our theoretical results help rationalize the experimental findings. A number of other viruses (such as HIV) also attach to cells through distinct receptors on the viral surface. Thus, our findings suggest criteria for fabricat-

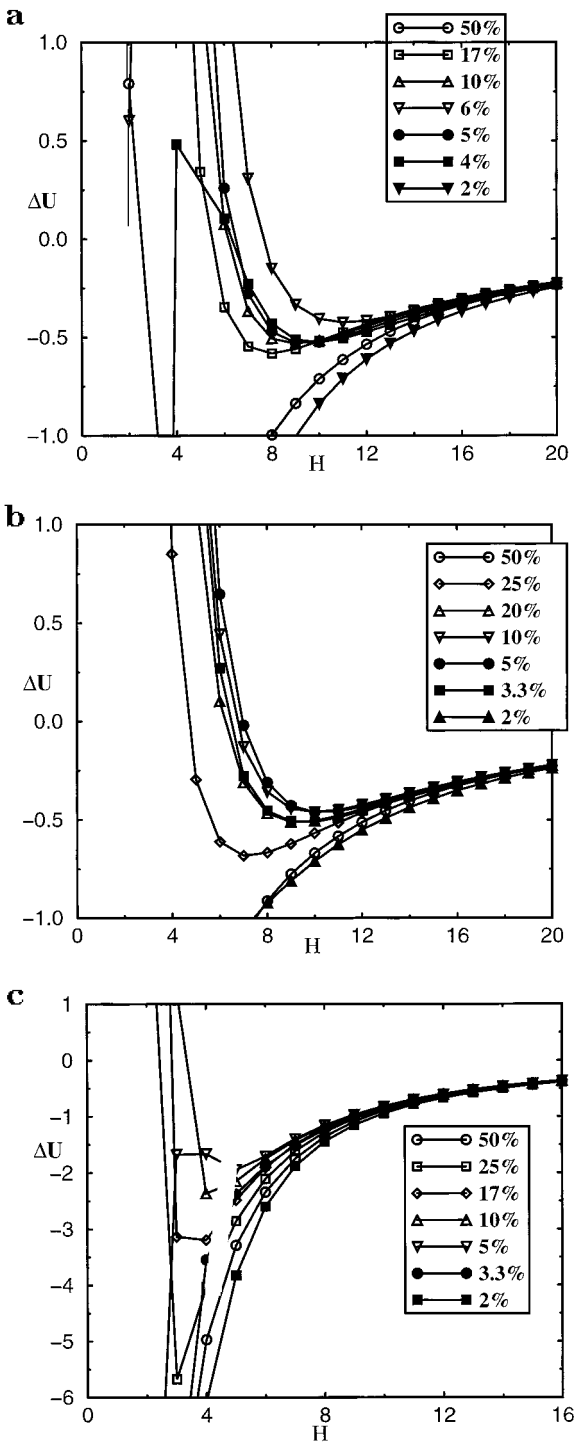

Figure 14. Interaction curves, ΔU vs H, for various sticker concentrations, c. Here, $\epsilon/kT = 7.5$ and $A/12\pi kT = 0.01$. The results are from the *sq* calculations. In part a, $d = 6$, and each receptor is one lattice site in size. In part b, $d = 6$, but each receptor occupies 2 contiguous sites. In part c, the distance between the two-site receptors is increased to 12 ($d = 12$).

ing effective polymeric inhibitors for a number of pharmaceutical applications.

In future studies, we will consider more detailed models for the structure of the virus and the cells. Here, we viewed the viral and cell surfaces as planes of comparable size. We will extend this work by taking into account not only the roughly spherical shape of the particles but also differences in the sizes of the colloids.

Acknowledgment. The authors gratefully acknowledgment helpful discussions with Prof. George Whitesides. A.C.B. gratefully acknowledges support from the ONR through grant N00014-91-J-1363, from the NSF, through Grant No. DMR-9709101, and from the DOE, through Grant No. DE-FG02-90ER45438.

References and Notes

(1) Napper, D. H. *Polymeric Stabilization of Colloidal Dispersions*; Academic Press: New York, 1983.
(2) Stryer, L. *Biochemistry*; W. H. Freeman and Company: New York, 1988; p 869.
(3) Wiley, D. C.; Skehel, J. J. *Annu. Rev. Biochem.* **1987**, *56*, 365.
(4) Wharton, S. A.; Weis, W.; Skehel, J. J.; Wiley: D. *The Influenza Viruses*, Krug, R. M., Ed., Plenum Press: New York, 1989; p 153.
(5) Spaltenstein, A.; Whitesides, G. M. *J. Am. Chem. Soc.* **1991**, *113*, 686.
(6) Sigal, G. B.; Mammen, M.; Dahman, G.; Whitesides, G. M. *J. Am. Chem. Soc.* **1996**, *118*, 3789.
(7) Mastrosovich, M. N.; Mochalova, L. U.; Marinina, V. P.; Byramova, N. E.; Bovin, N. V. *FEBS Lett.* **1990**, *272*, 209.
(8) Roy, R.; Laferriere, C. A. *Carbohydr. Res.* **1988**, *177*, c1.
(9) Mammen, M.; Choi, S.-K.; Whitesides, G. M. *Angew. Chem., Int. Ed. Engl.*, in press.
(10) The value of ϵ is on the order of $10kT$ for the binding of a SA group within a copolymer to the HA receptor. (Whitesides, G. M. Private Communication.)
(11) Russell, W.; Saville, D. A.; Schowalter, W. R. *Colloidal Dispersions*; Cambridge University Press: Cambridge, England, 1989; p 134.
(12) (a) Issaevitch, T. A.; Jasnow, D.; Balazs, A. C. *J. Chem. Phys.* **1993**, *99*, 8244 and references therein. (b) Zhulina, E. B.; Skvortsov, A. M.; Birshtein, T. M. *Polym. Sci. USSR* **1981**, *23*, 304. (c) Muthukumar, M. *J. Chem. Phys.* **1995**, *103*, 4723. (d) Andelman, D.; Joanny, J.-F. *Macromolecules* **1991**, *24*, 6040. (e) Srebnik, S.; Chakraborty, A. K.; Shakhnovich, E. I. *Phys. Rev. Lett.* **1996**, *77*, 3157.
(13) This specific conformation is a rather arbitrary choice; it is not a necessary condition of the model. Any conformation in which the chains form extended loops of relatively uniform size is also appropriate in this theory.
(14) Again, our choice of where to cut the loops is rather arbitrary. Within the framework of scaling theory, the cut can be made anywhere along the chain as long as the resulting fragments, or subchains, form extended tails of relatively uniform size.
(15) (a) Skvortsov, A. M.; Gorbunov, A. A.; Parlushkov, V. A.; Zhulina, E. B.; Borisov, O. V.; Priamitsyn, V. A. *Polym. Sci. USSR* **1988**, *30*, 1706. (b) We employ a mean-field approximation to describe the polymer coating. We use this approach in order to be consistent with our numerical SCF calculations. The use of a scaling model for the free energy will not lead to qualitative changes in the general picture.
(16) Alexander, S. *J. Phys. (Paris)* **1977**, *38*, 983.
(17) de Gennes, P.-G. *J. Phys. (Paris)* **1976**, *37*, 1443.
(18) (a) Singh, C.; Pickett, G.; Balazs, A. C. *Macromolecules* **1996**, *29*, 7559. (b) Pickett, G.; Balazs, A. C. *Macromol. Symp.* **1997**, *121*, 269.
(19) Decreasing the local solvent quality might not, however, be practical for in vivo applications.
(20) Fleer, G.; Cohen-Stuart, M. A.; Scheutjens, J. M. H. M.; Cosgrove, T. Vincent, B. *Polymers at Interfaces*; Chapman and Hall: London, 1993.
(21) (a) Huang, K.; Balazs, A. C. *Phys. Rev. Lett.* **1991**, *66*, 620. (b) Huang, K.; Balazs, A. C. *Macromolecules* **1993**, *26*, 4736. (c) Israels, R.; Gersappe, D.; Fasolka, M.; Roberts, V. A.; Balazs, A. C. *Macromolecules* **1994**, *27*, 6679.
(22) The area of our surface is equal to Σ. To compare the free energies per unit area in the *sq* and *cu* cases, we scale the corresponding *sq* results by a numerical coefficient. $\kappa = (2d + 1)/(d + 1)^2$. The latter procedure corresponds to superimposing a larger grid on an area Σ of the *sq* lattice, where the distance between grid points is now equal to d, the spacing between the receptors. We are effectively multiplying the *sq* free energy by the total number of sites that belong to the larger grid.
(23) Zagst, K. J.; Balazs, A. C.; Whitesides, G. M. In *Proceedings of the Sixth National Conference on Undergraduate Research*; Ed. Yearout, R. D., Ed.; University of North Carolina: Asheville, NC, 1992; Vol. 2, p 1201.

MA980624D